03,15

Megadevices of silicon microelectronics

© V.K. Eremin, E.M. Verbitskaya, N.N. Fadeeva

Ioffe Institute,
St. Petersburg, Russia

E-mail: elena.verbitskaya@mail.ioffe.ru

Received October 10, 2024
Revised November 17, 2024
Accepted November 18, 2024

New megadevices, such as particle detectors for experiments at the Large Hadron Collider, space gamma-ray telescopes, and detectors of dark matter particles and neutrinos, in which the scale of the silicon part of the apparatus goes beyond the usual understanding of a „semiconductor device", are described in terms of semiconductor physics, which will make it possible to assess specific problems of their implementation and development prospects due to the direct impact of fundamental science.

Keywords: silicon p^+-n-n^+-sensor, detector of events, Large Hadron Collider, gamma-astrophysics, neutrino.

DOI: 10.61011/PSS.2025.01.60573.1-25

1. Introduction

The challenges of fundamental science have a direct impact on the boundaries of the field in which semiconductor devices and their technology confidently occupy a leading position. This steady trend has continued in recent decades, when plans for fundamental high-energy physics have been consistently implemented along with the development of its instrumental base. The progress of fundamental research in high energy physics (HEP) and nuclear physics is a vivid example of the impact of science on the development of new technologies. The instrumentation of experiments on the study of the atomic nucleus, the Universe, and elementary particles in major international scientific centers required instruments that changed both the radiation-sensitive material and the principles of their operation. The evolution of the radiation sensor material is described by the sequence: gas — liquid — solid, including semiconductors. The principles of building the experiments varied depending on the tasks, from measuring the characteristics of a single particle (particle detectors) to recording complex events in the Microcosm (event detectors). The new scale of their characteristic energies required an appropriate amount of sensitive material and the detailed information about the geometry and kinetics of the process (i.e. 4D information). Accordingly, the previously existing instrument base built on gas and scintillation detectors needed to be complemented with new-generation detectors with compact size, time resolution of up to tens of ps, and coordinate resolution of few μm. The problem was solved by the large-scale application of silicon (Si) as a material for individual sensors for detectors, which are currently complex recording devices. In them, it is silicon that as a solid ensures the necessary probability of interaction of particles and quanta with the sensor sensitive bulk and is already used as a semiconductor in a wide range of devices for civil and industrial applications, for the production of which there is a powerful technological base. The latter practically opened up new experimental possibilities in the HEP driving the development of silicon megadetectors of events, which were created and are created with the participation of Ioffe Institute.

Undoubtedly, the largest megadetectors are the vertex silicon detectors of A Toroidal LHC ApparatuS (ATLAS) and Compact Muon Solenoid (CMS) experiments at the Large Hadron Collider (LHC) in CERN [1]. Future plans include the large-scale application of silicon to create sensors in gamma-ray telescopes and detectors of weakly interacting particles, which include particles responsible for the existence of dark matter — the so-called weakly interactive massive particles (WIMPs) and neutrinos. These examples illustrate the new opportunities opening up for HEP, astrophysics, and nuclear physics based on the use of silicon microelectronics technologies. It should be noted that the term „detector" used below defines fully functional devices, which include particle detectors and event detectors, while sensors or sensitive elements are an integral part of the latter.

2. Historical note

Semiconductor nuclear radiation detectors were created in the 1960s and are still a type of device in demand that successfully solves the problems of nuclear science and technology. The physics of their functioning describes all the processes accompanying the particle detection, starting from its interaction with silicon, the subsequent drift of nonequilibrium charge carriers (NCC) generated by a particle in a sensitive bulk, and the formation of an electrical signal at the detector contacts as a response to

the detected particle by means of electrostatic induction. These processes should ensure proportionality between the energy of the detected particle and the charge induced on the detector contacts, provide a low noise level and long-term stability of these characteristics. The development of silicon detectors was based on metal-semiconductor-metal structures until the 1980s, which demonstrated the potential of semiconductor detectors and at the same time revealed their serious drawbacks — the values of the dark current and the corresponding signal-to-noise ratio exceeding the estimate based on the characteristics of silicon. The low reproducibility of the technological process limited the mass production of identical detectors and reduced the scope of tasks to the spectrometry of individual particles, despite their undoubted advantages over gas and scintillation detectors.

The importance of detection of particle tracks and events, i. e. processes involving multiple particles, arose already at the beginning of the 20th century, the history of which is described in Ref. [2]. Created in 1912, the so-called „cloud chamber“ (C.T.R. Wilson, Nobel Prize in Physics 1927) in which particles left traces of superheated steam droplets through which they moved, made it possible to visualize the tracks of particles and the event itself. A significant step in the development of this principle, which consists in changing the aggregate state of a sensitive substance along the path of particle movement, was the replacement of a gaseous working medium with a liquid („bubble chamber“ — D. Glaser, 1957 Nobel Prize in Physics) which, starting with 1953, remained the main tool in the HEP for more than 20 years. The volume of bubble chambers has reached $3.7\,\mathrm{m}^3$ in recent R&D (Large European bubble chamber at CERN, working medium — liquid hydrogen or other gases with heavier molecules, which increased the stopping power of the detecting medium).

Along with undoubted advantages, bubble chambers had a serious drawback: they were slow event detectors and did not allow obtaining information about the kinetics of processes. Therefore, the introduction of position-sensitive Si sensors with high coordinate and time resolution became the basis for the next generation of event detectors and advanced significantly the capabilities of experimental HEP. Their development is directly related to the use of planar technology processes to create large-area p^+-i-n^+-Si detector structures and ion implantation techniques for doping thin contact layers [3]. As a result, sensor characteristics have been stabilized, dark currents have been reduced by more than an order of magnitude, and precision segmentation of contact areas became possible. It was also important that the high controllability of technological processes made it possible to reduce the sensor characteristic spreading, which is important for creating complex detection structures.

3. Microstructures of silicon planar sensors

Signal generation in silicon sensors based on p^+-n or n^+-p-junction (where p^+ and n^+ are heavily doped contact layers) is associated with the transfer of nonequilibrium charge carriers generated by incident particles, and is determined according to the Shockley-Ramo theorem by the magnitude of the current i during the movement of the charge q at a point with the coordinate x at a time t [4]:

$$i(x) = qF_w(x)\mu(F, T)F(x),$$

where μ is the carrier mobility depending on the electric field F and temperature T, x is the coordinate normal to the sample surface, and F_w is the weighting electric field, having dimension cm^{-1}. F_w is calculated as the field at the location of the charge when the voltage $V = 1\,\mathrm{V}$ is applied to the detecting contact and the other contacts are grounded. The one-dimensional approximation provides an adequate description of the current for an unsegmented sensor with two plane-parallel contacts with their linear dimensions exceeding the thickness of the structure d and charge movement in the direction perpendicular to the contacts; in this case, $F_w = 1/d$. F_w is a two-dimensional or three-dimensional function for segmented sensors that depends on the geometry of the contacts and the trajectory of the charge [5], and the current is calculated by modeling using modern software packages. The current signal is integrated by a charge-sensitive amplifier and is supplied to the input of the readout electronics.

The types of structures of planar Si sensors, their characteristics, and application for detecting various radiations are described in detail in Refs. [5–9]. The classification of planar structures includes non-segmented (pad) sensors of various sizes and segmented sensors such as strip and pixel sensors, with different topology of segmentation of p^+-n- or n^+-p-junctions to ensure their positional sensitivity. Strip structures are designed with segmentation of one side — single-sided strip detectors (SSSDs) or both sides — double-sided strip detectors (DSSDs); the latter have 2D sensitivity. A further improvement in positional sensitivity is achieved in pixel sensors obtained by strip segmentation.

The main requirements for modern silicon sensors are provided in the table.

The combination of requirements leads to the need to introduce several special elements into the design of a silicon sensor, which are briefly described below. One of the most important requirements is the extremely low value of the dark current at a high operational voltage V, which is necessary to achieve a large thickness of the sensitive region and efficient and fast collection of NCC generated by the detected particle. The sensors exposed to radiation in the LHC experiments are the most critical for meeting these conditions, since local regions with high electric field can arise in their structure at operational voltages of hundreds of volts.

Characteristics and requirements for Si sensors

Characteristic	Requirement	Value
Sensitive area	Creation of detection surfaces with large area	Up to 100 cm^2
Thickness of the sensitive area	Full or sufficient absorption of energy of the detected particle to measure its magnitude	10^{-3}–10^{-1} cm
Dark current generated in the sensitive area	Detection of weakly absorbed radiation or low-energy particles	10^{-10}–10^{-9} A/cm^2
Efficiency of NCC collection	Accuracy of determining the energy released by a particle in a sensitive volume	99.9%
Time resolution	Time characterization of the studied process	$< 10^{-10}$–10^{-8} s
Operational voltage	Full depletion of sensitive volume, efficient collection of NCC, the shortest signal, high time resolution	100–1000 V
Operational temperature	Improved sensitivity and time resolution, reduction of noise and energy release	−(10–20)°C (CERN-ATLAS)
Long-term stability of characteristics without taking into account radiation effects	Long-term experiments without the possibility of replacement of detectors during the operation period	Several years

Creation of a peripheral potential divider is an effective way to reduce the impact of the silicon device chip boundaries on its characteristics. Such structures, discussed in Refs. [10,11], are widely used in pulse power semiconductor electronics devices to prevent avalanche breakdown of shallow electron-hole junctions and silicon nuclear radiation sensors designed for operation at high voltages. The divider for sensors processed on high resistivity n-Si (p^+–n–n^+-structure) is formed by a series of closed „floating“ p^+-rings separated by insulating inter-ring gaps, the surface of which is passivated with SiO_2 film (Figure 1). This stabilizes the current-voltage characteristic of the sensors, which makes it possible for them to operate in fully autonomy mode without the possibility of replacement in the experiments in space and HEP with a duration in years. In the above fields, the creation of such structures has become possible thanks to advances in microelectronic technologies.

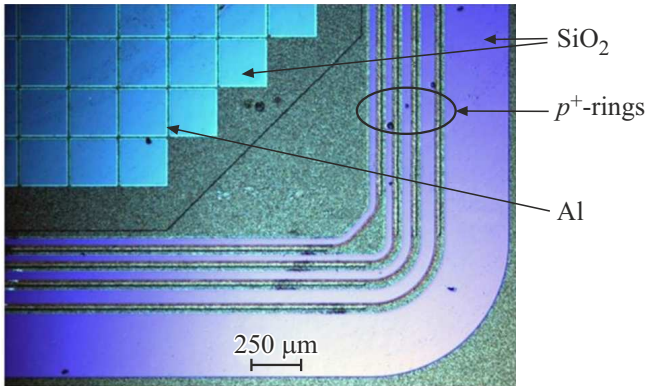

Figure 1. Photo of a fragment of the surface of a silicon sensor with a ring system of a peripheral potential divider.

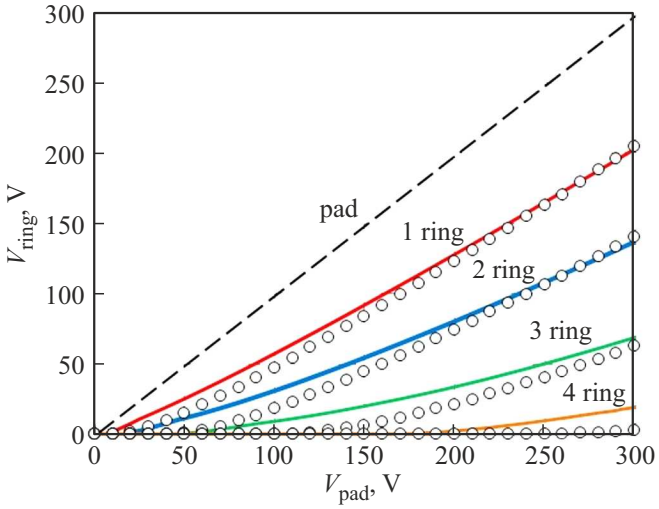

Figure 2. Distribution of potential on ring p^+–n-junctions in a detector based on n-silicon with a resistivity of 5 kΩ·cm: symbols — experiment, solid lines — calculation, dashed line — potential at the central (pad) p^+-contact.

The rings work as a system of isolated p^+–n-junctions, the potential of which is determined by the condition of the current flow in the inter-ring gaps generated in the depleted region of the ring junctions [12]. The results of measurements and numerical calculation of the potential of p^+-rings depending on the voltage V_{pad} applied to the central p^+-contact (the so-called pad contact) are shown in Figure 2. The distribution of potentials over the divider rings and the currents flowing between them are self-consistent and set automatically, which ensures the sensor stability. It can be seen that the ring divider operates over the entire voltage

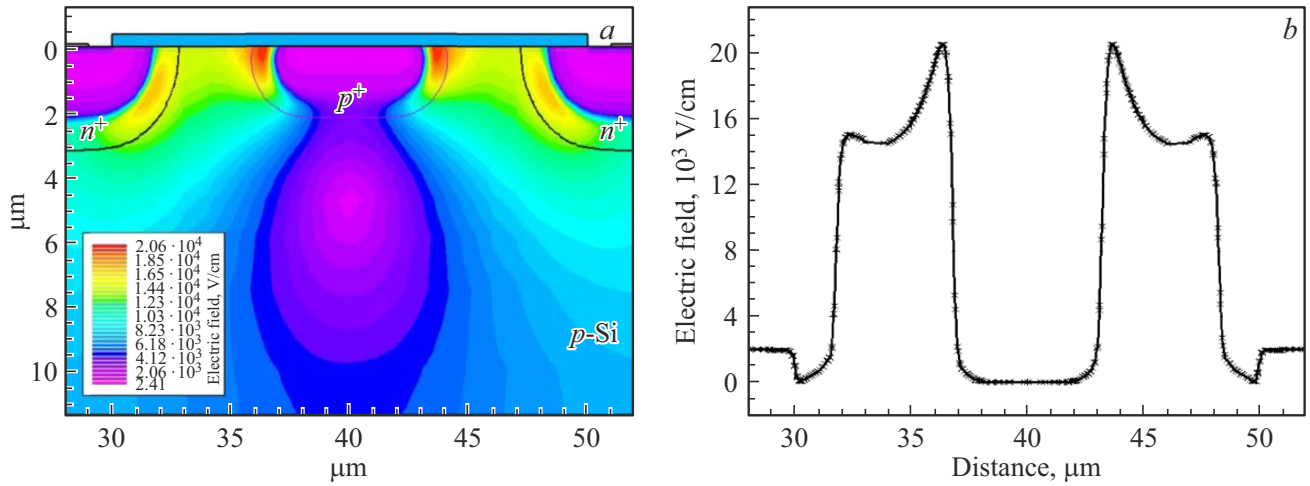

Figure 3. *a* — 2D distribution of the electric field in the interstrip gap of n^+-p-p^+-sensor and *b* — distribution of the electric field at a depth of $0.1\,\mu$m from the surface. $V_{pad} = 150$ V.

range applied to the central p^+-contact, and the potential in the ring structure varies gradually between the sensitive region and the sensor periphery, without creating areas with high electric field. Figure 2, as well as 3 and 4 (below) represent the authors' results.

The radiation exposure to p^+-n-n^+-sensors in experiments at the LHC leads to the accumulation of radiation defects, the concentration of which is maximum for acceptor-type defects. At a certain critical dose this leads to the transformation of high-resistivity *n*-Si into high resistivity *p*-Si overcompensated by deep acceptors. Deep acceptors and donors are recharged in the sensor's operational mode, i. e. at reverse voltage and dark generation current flowing in the depleted region, the result of such recharging is determined by their position in the silicon bandgap and the charge carrier capture cross section [7]. Accordingly, the sign of the space charge is inverted at radiation doses above the critical dose and becomes negative, and the electric field maximum moves to the n^+-contact, which increases the efficiency of collecting electron charge at n^+-contact segments and improves sensor timing performance.

Therefore, modern position-sensitive sensors used in experiments at CERN are manufactured as n^+-p-p^+-structures based on high resistivity *p*-Si and segmentation of n^+-contact located in the region of high electric field at any radiation dose [13]. In such sensors, regardless of the dose, a signal is formed at the n^+-contact, which makes their operation more predictable, excluding the point of space charge sign inversion in the scenario. However, in this case, the interstrip insulation and the insulation of the rings of the potential divider require interruption of the conductivity layer of electrons accumulated in *p*-Si under the Si—SiO_2 interface, resulting from the built-in positive charge in the oxide ($\sim 10^9-10^{10}$ cm^{-2}). An effective way to interrupt the link between n^+-sensor segments is to introduce separation p^+-regions into the intersegment gaps — the so-called *p*-spray or *p*-stop, in which the concentration of acceptors significantly exceeds the concentration of accumulated electrons [14].

Figure 3, *a* shows the distribution of the electric field *F* in the interstrip gap in a sensor based on *p*-Si at a voltage $V_{pad} = 150$ V. The width of the p^+-region and the distances between n^+-strips are 10 and 5μm, respectively. It can be seen that region with an electric field is formed under the p^+-layer, destroying the layer of accumulated electrons, which prevents the flow of current between the n^+-strips. In this case, maxima of 20 kV/cm arise in the distribution of electric field at the boundary of the p^+- layer (Figure 3, *b*).

A similar isolation principle is used in the ring potential divider of sensors based on *p*-Si. Figure 4, *a* shows the distribution of the dopant concentration in the topology-optimal n^+-p-p^+-structure with a potential divider consisting of eight n^+-rings with the inclusion of insulating p^+-regions between them (the latter are located under SiO_2 layers, indicated in blue) when voltage $V_{pad} = 500$ V is applied.

It can be seen from the distributions of potentials between the rings and the electric field (Figure 4, *b* and *c*) that the potential decreases stepwise from 500 V at the sensitive area element to 100 V at the last n^+-ring. The distribution *F* at the boundaries between the insulating p^+-regions under the oxide and n^+-rings is more complex than in the interstrip gap (Figure 3), and its structure and the position of the field maximum are sensitive to the location of the boundaries of p^+-elements and metallization.

Figure 5 shows an example of the implementation of the elements discussed above in a mini-prototype of n^+-p-p^+-sensor with a strip pitch of 65 μm, developed in Ioffe Institute for the TOTEM experiment at the LHC.

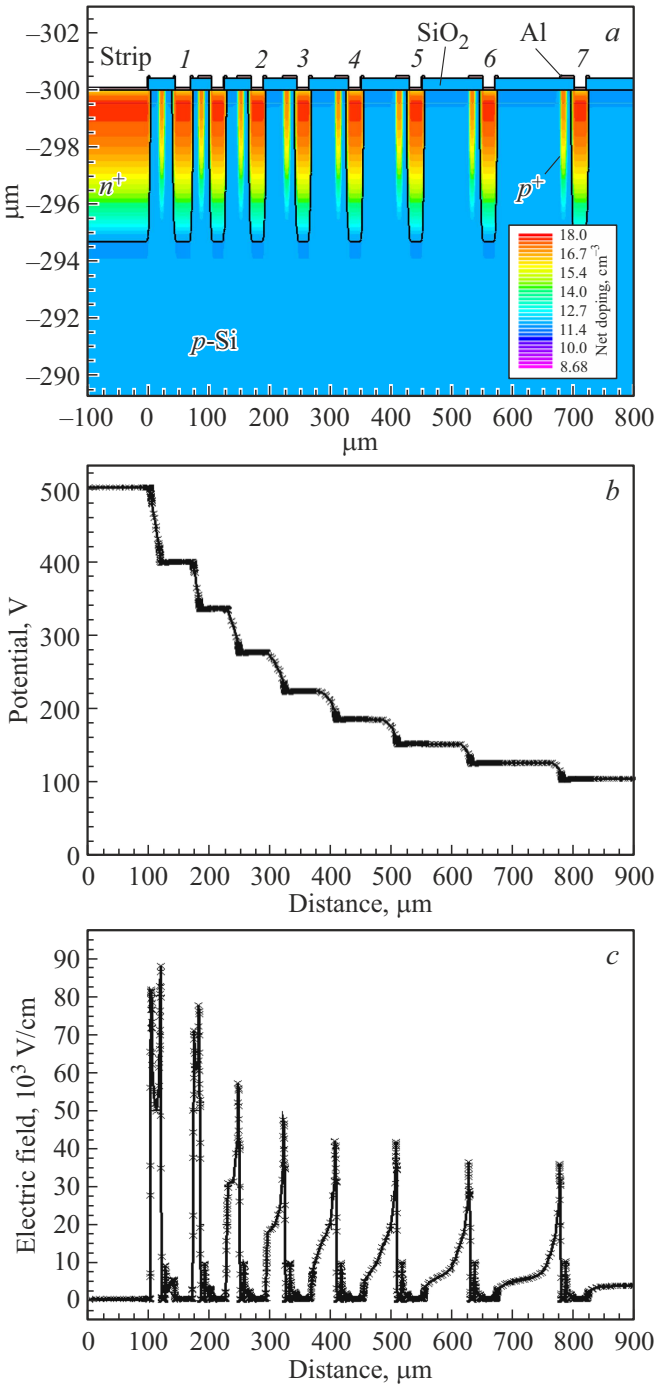

Figure 4. Distribution a — dopant concentration, b — potential and c — electric field in n^+-p-p^+ sensor with potential divider. $V_{pad} = 500$ V.

It should be noted that what is specific to position-sensitive sensors is their super-large size, reaching $10 \times 10\,cm^2$, compared with digital electronics chips with hundreds times smaller size. In this case, the contours of elements such as strips and rings of potential dividers can have a length of up to 0.4 m and be separated from each other by a distance of μm, which is a non-standard requirement for planar technology, which distinguishes nuclear radiation detectors as a unique class of devices.

4. Modern and planned megadetectors based on silicon sensors

Examples of critical elements of modern silicon sensors have shown the importance of microstructures and their design, and the need to use planar silicon microelectronics technology in the development of this type of devices for experimental HEP. The achieved and planned results related to the creation of Si event detectors in the largest experiments are presented below using the examples of the ATLAS experiment detector at CERN, as well as plans to build space gamma-ray telescopes. The neutrino research project is an example of a project requiring a large-mass silicon megadevice (sec. 4.3). Its creation is not related to the use of microelectronic technology, however, the detector itself can be attributed to unique silicon mega-devices for detecting nuclear radiation, which motivated its brief description in this paper.

4.1. Silicon megadetectors in HEP: inner tracker of ATLAS experiment

The instrumental base of experiments at the LHC is the most striking example of the creation of silicon-based megadetectors. The program of LHC upgrade provides for its phased transformation into a high-luminosity large hadron collider (HL-LHC) with the following proton beam

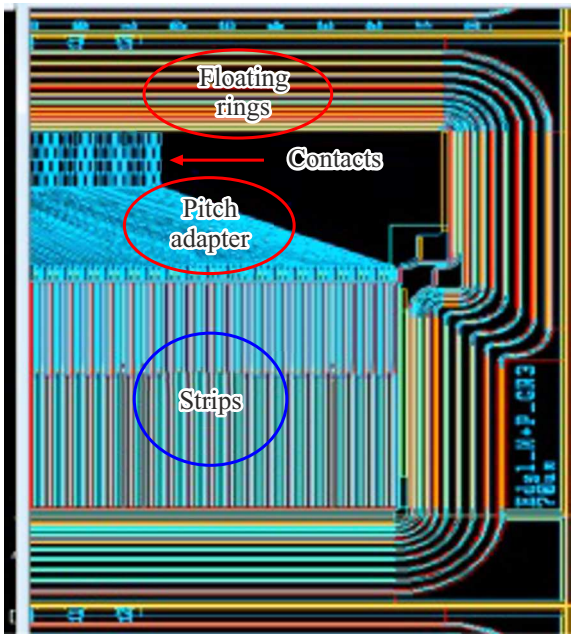

Figure 5. The topology of a fragment of the mini-prototype of n^+-p-p^+-sensor developed in Ioffe Institute with a strip pitch of 65 μm, a ring potential divider consisting of n^+-rings, a pitch adapter and contact pads.

characteristics: proton energy of 13 TeV, increase of luminosity from $\sim 10^{34}$ to $7.5 \cdot 10^{35}$ cm^{-2}s^{-1} and the maximum radiation dose from $5 \cdot 10^{14}$ to $2 \cdot 10^{16}$ n_{eq}/cm^2. The specific feature of silicon sensor operation in long-term experiments at CERN is their degradation under the impact of detected and background radiation; therefore, many of them are constantly upgraded in 2 aspects: the use of p-Si as the optimal material for sensors and the creation of their new designs.

ATLAS is one of the largest international multi-purpose experiments conducted at CERN and intended to study proton-proton collisions and search for superheavy elementary particles such as the Higgs boson and supersymmetric partners of Standard Model particles [15]. In general, the ATLAS multilayer detector is a cylinder with a length and diameter of 46 and 25 m, respectively. An inner semiconductor tracker is located in the immediate vicinity of the proton collision point, which has a length of 5.6 m and was built on the basis of Si sensors with an active area of 61 m^2 at the initial stage of the experiment. The tracker's tasks are to measure the direction of motion, momentum and charge of electrically active particles produced in each collision of protons of oncoming beams. The characteristics and design of the silicon inner tracker were already unique at the time of its launch in 2007, both in terms of technical characteristics, including electronics, and particle detection capabilities, and were a new step made owing to advances in silicon microelectronics.

Currently, the ATLAS inner tracker includes layers of pixel sensors closest to the proton interaction point (Figure 6, [16]). The sensors have 2D sensitivity and ensure spatial resolution of 10 μm. The layers of sensors with short and long strips are the next after the pixel sensors, which ensures the accuracy of determining the trajectory of a particle passing through the sensor in 20 μm and, together with an array of pixel sensor data, provides information about the proton collision point with an accuracy of μm.

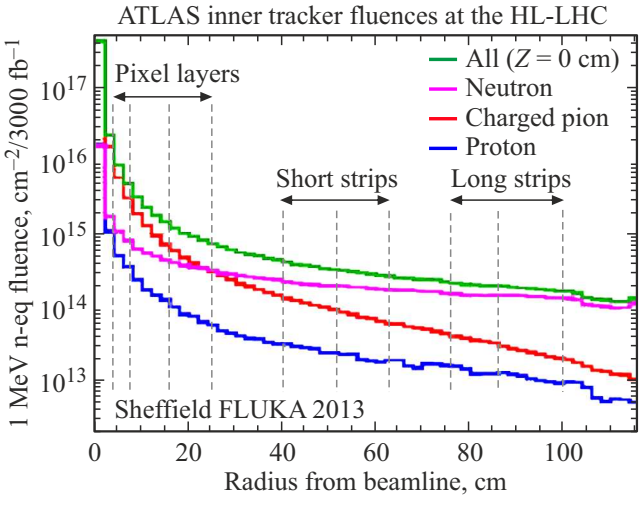

Figure 6. Expected radiation doses of silicon sensors in the inner tracker in ATLAS experiment at HL-LHC [16].

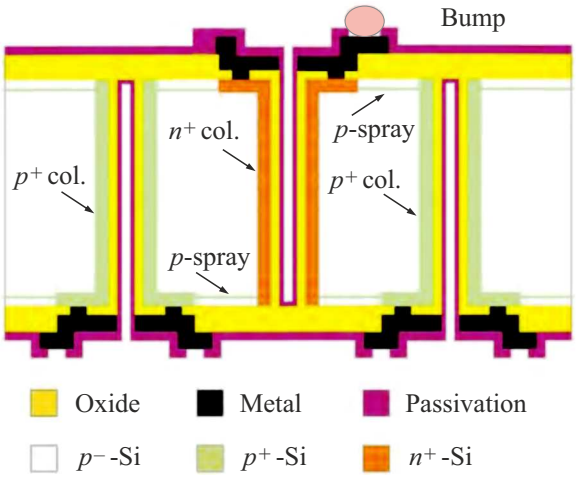

Figure 7. Schematic representation of a 3D pixel sensor based on p-Si [18].

In HL-LHC, the maximum radiation dose of sensors should increase to $2 \cdot 10^{16}$ n_{eq}/cm^2, which is taken into account in the tracker upgrading plans. At the same time, basing on the results on the radiation degradation of Si detectors obtained by the RD50 collaboration and researchers participating in the LHC experiments, there is no reason to expect progress in increasing the radiation hardness of the bulk silicon itself. Therefore, the development of tracker sensors is associated with the creation of new designs that implement sensor topologies optimal for signal formation.

In particular, the design and characteristics of strip sensors have been improved, and an additional inner layer of the tracker has been introduced, including sensors based on the vertical structure of p–n-junctions processed using 3D technology (Figure 7) [17,18]. Heavily doped layers are made as the columns (n^+-col. and p^+-col.) in n^+–p–p^+-sensor shown in the figure, and the p-spray layer ensures their electrical insulation in the subsurface layer. It is also planned to use sensors with low signal gain — the so-called low gain avalanche detectors (LGAD) in the tracker, which will improve the time resolution to 30–50 ps [19]. Accordingly, the number of signal readout electronics channels has increased significantly (to $92 \cdot 10^6$ in 2023), and as a result, better coordinate resolution has been obtained for track reconstruction and time resolution for studying the kinetics of particle motion.

4.2. Silicon microelectronics megainstruments for gamma-ray astrophysics

A global task in gamma-ray astrophysics is to determine the location of the gamma radiation source, for which telescopes using scintillation detectors have been a traditional tool. The requirements for the elements of telescopes are in many ways similar to those put forward for devices at CERN — measurement of the initial or formed particles energy, high spatial and time resolution, as well as a wide

field of view of the studied area of outer space. In turn, the radiation hardness of the equipment used is not relevant due to the small cross-section of the interaction of cosmic particles with the recording medium. Therefore, silicon sensors with a p^+-n-n^+-structure can be used for gamma-ray astrophysics tasks, which simplifies building telescope elements, the main of which are a tracker and a calorimeter.

The most important processes occurring during the passage of gamma quanta through matter are [6]:

- the Compton effect — scattering of a gamma quantum on an electron; as a result of each interaction of a quantum with an electron, the energy of the quantum E_γ and the direction of its movement change, which allows determining the angle of its incidence on the telescope,
- generation of electron-positron pairs ($e-e^+$) in the electric field of the nucleus, efficient at $E_\gamma > 10$ MeV.

The multi-stage process of a gamma quantum registration using the Compton scattering mechanism, which makes it possible to determine the energy and reconstruct the direction of its movement towards the telescope, is illustrated in Fig 8. In a two-stage process, a gamma quantum incident on the surface of the tracker at an angle of θ with an energy of E_γ experiences Compton scattering on an electron in one of the tracker sensors, forming a recoil electron with an energy of E_1 and reducing its energy up to $E_\gamma - E_1$. The scattered gamma quantum, continuing to move in a new direction, has a chance to re-scatter on the electron at another point in the tracker, transferring to it the energy E_2, and once again change the energy and direction of movement.

The expression relating θ and energy losses E_1 and E_2 in scattering acts allows determining the angle of incidence of the gamma quantum on the telescope [6]:

$$\cos\theta = 1 - m_e c^2 \left(\frac{1}{E_2} - \frac{1}{E_1 + E_2} \right),$$

where $m_e c^2 = 511$ keV is the energy equivalent of the electron rest mass. In the two-stage process, E_γ is measured as the integral of the charges generated in the sensor layers of the tracker; in the three-stage process, the energy measured by the calorimeter, in which the gamma quantum releases the remaining energy, is added to this value.

The most famous space gamma-ray telescope was the Imaging Compton Telescope (COMPTEL), which was part of the Compton Gamma Ray Observatory [20]. The telescope carried out studies based on the Compton effect in the energy range of 1–30 MeV and included 2 layers of scintillation detectors. The characteristics realized in the measurements on the telescope in 1991–2000 still remain the standard for comparison with estimates of parameters in telescopes planned for the future.

The current operating telescope using Si sensors is the Large Area Telescope (LAT) of size $1.8 \times 1.8 \times 0.72$ m^3 at the Gamma-ray Large Area Space Telescope (GLAST, now FGST or FGRST) space observatory, designed to study radiation in a wide energy range of 20 MeV–300 GeV [21]. The telescope's tracker detects electrons or $e^- - e^+$-pairs using

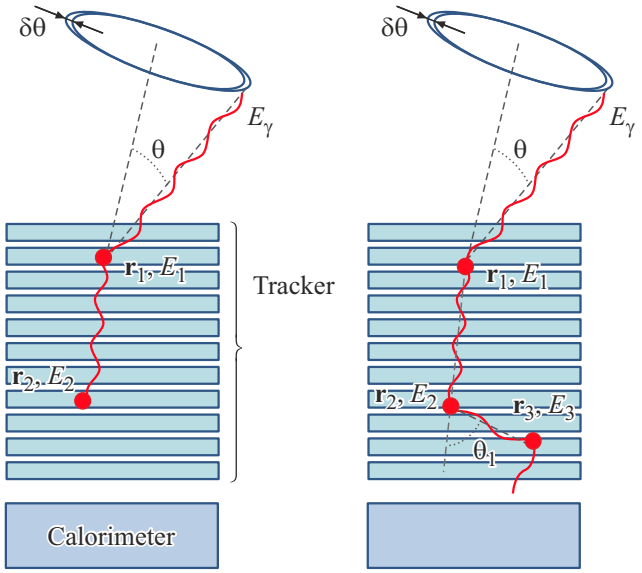

Figure 8. Schematic representation of the Compton process of gamma quantum detection in a gamma-ray telescope: left — a two-stage process with complete absorption of quantum energy E_γ in acts 1 and 2, right — a three-stage process with partial absorption of quantum energy in the tracker. r_j $(j = 1, 2, 3)$ is a vector defining the point where the scattering occurred.

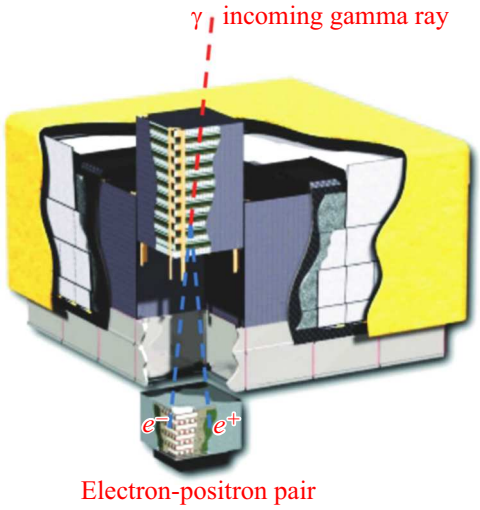

Figure 9. Schematic image of the gamma-ray telescope LAT [21].

single-sided strip sensors with an area of 8.95×8.95 cm^2, a thickness of 400 μm and a strip pitch of 228 μm. The sensors consist of 16 two-layer modules, each of them includes a vertical set of 18 SSSDs planes with mutually perpendicular strips (Figure 9), which ensures a 2D resolution. SSSDs register the passage of charged particles by measuring the tracks of generated $e-e^+$-pairs, which determines the location of the incident gamma ray source.

One of the most important results obtained was the registration of gamma-ray emission from an active galaxy

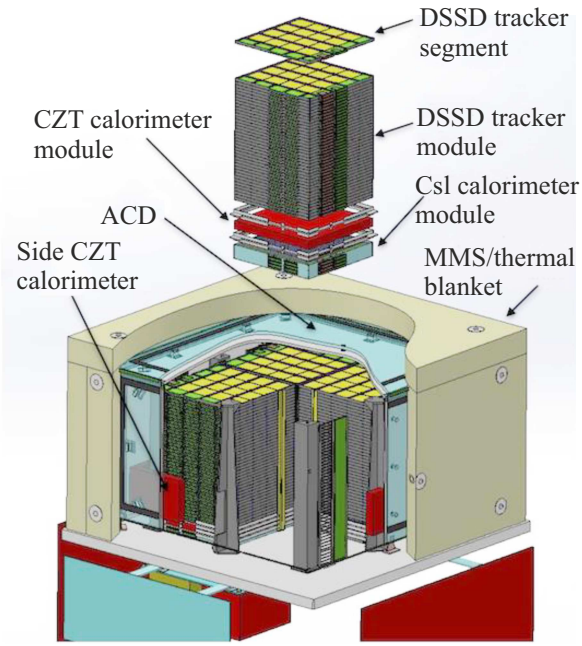

Figure 10. Schematic representation of the detection devices of the AMEGO telescope [23].

in combination with the detection of high-energy neutrinos from the same direction as detected by the IceCube neutrino detector; this fact for the first time showed the link between neutrinos and gamma-ray emission from an active galaxy [22]. The continuation of the FGRST observatory mission was approved by the US National Aeronautics and Space Administration (NASA) in 2019.

The planned international observatories All-sky Medium Energy Gamma-ray Observatory (AMEGO) [23] and enhanced ASTROGAM (e-ASTROGAM) [24] are expected to expand the scale of Si sensors application and use more advanced designs to improve energy and positional sensitivity. The energy of the studied gamma quanta will range from 0.3 MeV to more than 10 GeV and 0.3 MeV–3 GeV for AMEGO and e-ASTROGAM, respectively, i. e. the lower energy limit is shifted to the energy range of 200–300 keV compared to the LAT telescope, which is relevant for astrophysics. Both telescopes will contain 3 main units — a calorimeter based on scintillation crystals, a silicon tracker built as modular assemblies (towers) of sensors and an anti-coincidence system. The trackers will be built as modules combining DSSDs layers, creating a 3D space that allows to register events occurring in it with reference to a time scale. Thus, in the AMEGO telescope the tracker consists of 4 modular assemblies, each of these contains 60 layers, including 4×4 DSSDs (Figure 10). The individual sensor has the shape of square $\sim 10 \times 10\,\text{cm}^2$ with thickness of $500\,\mu\text{m}$ with 192 strips on each side totaling to 370,000 strips. Work is currently underway for optimizing DSSDs for reducing dark current and interstrip capacitances [25]. The energy resolution in the MeV range is expected to improve by more than 20 times compared to the COMPTEL telescope.

The concept of the e-ASTROGAM observatory with a total weight of 1.2 tons is based on the results of numerical modeling, which assess the expected characteristics, and an analysis of possible problems [24]. It is planned that the silicon tracker of electrons and $e^- - e^+$-pairs will contain 90 DSSDs layers with a layer area of $\sim 1\,\text{m}^2$, i. e. the total area of silicon sensors will be $\sim 90\,\text{m}^2$ with 860000 independent channels, which even exceeds the area of Si sensors in the inner tracker of the ATLAS detector. The area of each DSSD with a thickness of $500\,\mu\text{m}$ and a strip pitch of $240\,\mu\text{m}$ will be $9.5 \times 9.5\,\text{cm}^2$. Thus, the concepts of the AMEGO and e-ASTROGAM telescopes are based on the rich heritage of the LAT telescope and innovative technologies for manufacturing silicon strip sensors developed for the HEP.

The potential of Russia, including potential of the Ioffe Institute, in the field of fundamental gamma-ray astrophysics and the development of a silicon-based detection device is expected to be combined in a telescope project for detecting gamma quanta with energies of 0.3–10 MeV. Limiting the range of studies to an energy of 10 MeV allows abandoning the calorimeter and thereby improving the weight characteristic of the telescope (no more than 350 kg). It is planned that the tracker will include 100

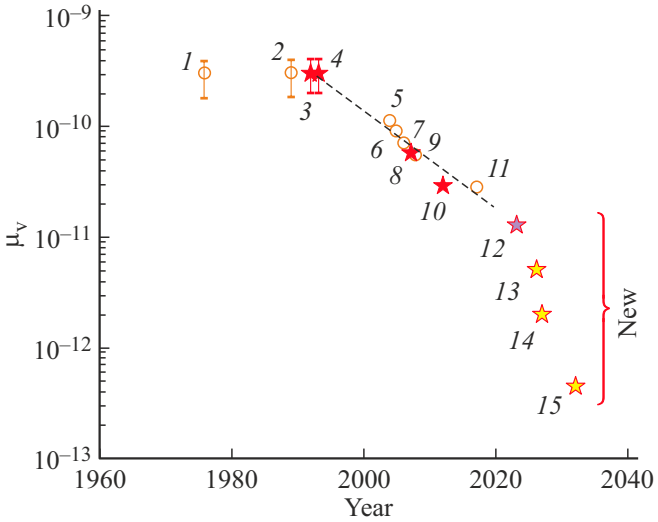

Figure 11. Progress in measuring the laboratory limit on the magnetic moment of an electron neutrino [27]. The following experiments are indicated by numbers: *1* — Savannah River (1976); *2* — Vogel, Engel (1989); *3* — National Research Center Kurchatov Institute (1992); *4* — Rivne, reactor (1993); *5* — Super-Kamiokande (2004); *6* — MUNU, reactor (2005); *7* — Texono collaboration, reactor (2006); *8* — GEMMA-I, reactor (2007); *9* — BOREXINO (2008); *10* — GEMMA-1, reactor (2012); *11* — BOREXINO, Gran Sasso (2017); *12* — GEMMA-2, reactor (2023–2024). New projects: *13* — Sarov, CsI detector (2026); *14* — Sarov, Si detector (2027); *15* — Sarov, helium detector (2030–2032).

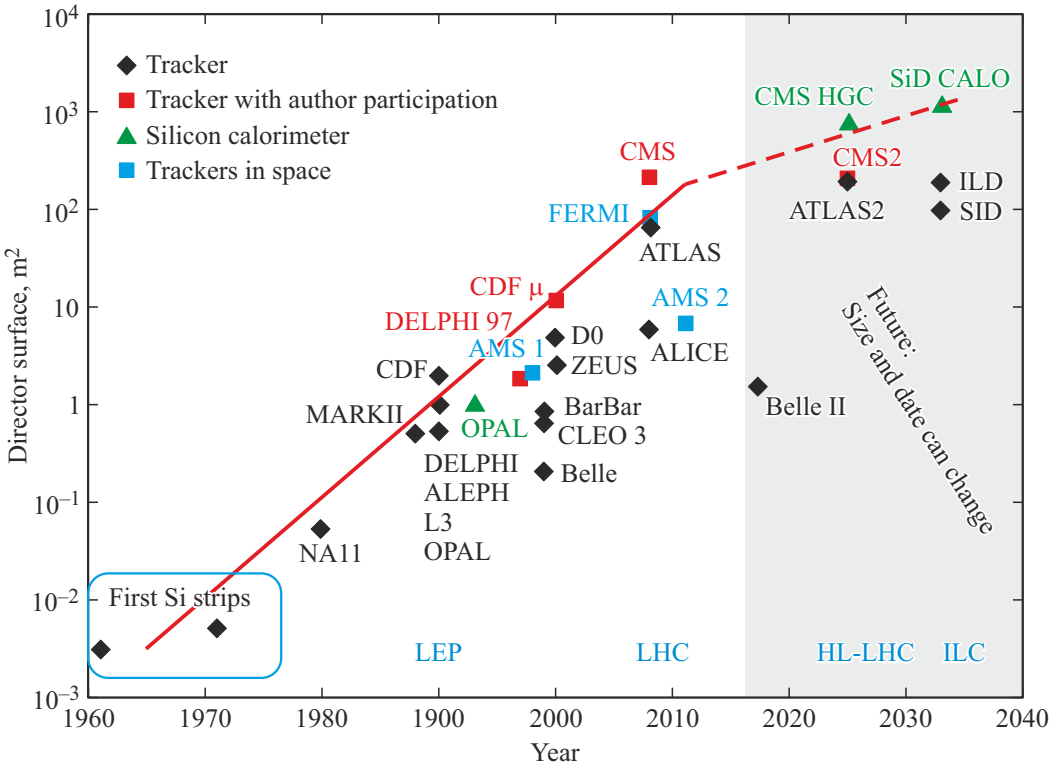

Figure 12. Evolution of detection systems in HEP and astrophysics [5].

layers of silicon strip p^+-n-n^+-sensors with an area of $\sim 10 \times 10\,\text{cm}^2$, providing 2D sensitivity.

A comparison between the parameters of the structures used in the topology of silicon sensors developed by the researchers of the Ioffe Institute and the parameters of the DSSDs planned for the e-ASTROGAM observatory clearly shows the possibility of implementing the required characteristics of the Si tracker in the Russian telescope. It is expected that the energy sensitivity will be 20–30 times better than that in the COMPTEL telescope.

4.3. Projects in the field of dark matter and neutrino research

The nature of dark matter and the properties of neutrinos are among the pressing issues of modern physics. Progress in reducing the laboratory limit on the magnetic moment of electron neutrinos of cosmic origin or emitted by nuclear reactors or tritium sources is shown in Figure 11. It can be seen that its value decreases down to $\sim 5 \cdot 10^{-13}\,\mu_B$ (where μ_B is the Boron magneton) in the planned new experiments.

The Cryogenic Dark Matter Search (CDMS/SuperCDMS) collaboration studies the scattering of dark matter particles using silicon sensors. The first experiments were performed on test samples with a mass of $\sim 1\,\text{g}$ at a temperature of 65 mK [26], and the long-term plans of SuperCDMS include the creation of a recording system with a total mass of 30 kg.

A new experiment using a unique silicon detector weighing 160 kg (No. 14 in Figure 11) is planned as part of program No. 8 of the National Center for Physics and Mathematics (NCPM) [27] and it will be conducted with the participation of several institutes at the site of the All-Russian Scientific Research Institute of Experimental Physics (VNIIEF), Sarov. The objective of the Ioffe Institute is to develop a silicon neutrino detector with an operational temperature of several tens of mK. In this experiment it is planned to use an intense tritium neutrino (antineutrino) source based on the reaction

$$^3_1\text{H} \rightarrow {}^3_2\text{He} + \text{e}^- + \bar{\nu}_e.$$

Taking into account the need to select neutrino-silicon interaction events and exclude background events, the detector should have a three-dimensional segmentation and consist of 1600 Si sensors weighing about 100 g each. The target characteristic is the threshold of sensitivity to the magnetic moment of neutrinos with a value of $\sim 2.5 \cdot 10^{-12}\,\mu_B$, which is an order of magnitude better than the value achieved in the GEMMA-2 experiment using sensors based on high-purity germanium.

In the experiment, it is planned to use the bolometric principle of particle registration, when the sensor signal is a pulsed change of its temperature due to the transfer of part of its energy by the particle to the sensor and the generation of Joule heat in it during the flow of the drift current of the NCC (the Neganov-Trofimov-Luke effect [28]). For

achieving the maximum signal-to-noise ratio, it is proposed to measure the temperature signal from the sensor with a transition edge sensor (TES) thermometer at the point of maximum steepness of the temperature dependence of its resistance.

It should be noted that cooling a silicon sensor to a temperature of tens of mK turns its sensitive bulk practically into an insulator, preventing the possibility of the formation of a space charge in it due to the emission of electrons and holes from shallow levels of dopants (phosphorus and boron) in *n*-Si, that takes place at temperatures below 4 K [29]. At the same time, the dopant purity of silicon and the low concentration of equilibrium phonons will ensure high mobility of charge carriers, and the absence of a space charge in the sensitive region will allow for the drift transfer of electrons and holes over distances measured in centimeters. Therefore, the detector being created provides for the possibility of applying a voltage of several hundred volts to its sensors for an internal thermal amplification of the signal owing to the release of Joule heat during the drift of nonequilibrium carriers formed by neutrinos. The first experimental studies of Si sensors at a temperature of ≤ 100 mK and with an application of voltage demonstrated that silicon in a sensitive bulk actually has the properties of a semiconductor close to an electrically neutral insulator, but with high mobility of electrons and holes [30], which is necessary for creating sensors with internal thermal gain for the neutrino detector.

5. Conclusion

It is obvious from the above that the operating silicon megadetectors are certainly the internal trackers in the HL-LHC experiments. Their development consists in the continuous advance of Si sensor designs to improve the positional resolution during particle detection and increase radiation hardness. The confirmation of the correctness of this trend is the outstanding discovery of the Higgs boson based on the results obtained in the ATLAS detector. The evolution of detecting Si systems in HEP and astrophysics and the extrapolation of their development for the next 16 years (as it was imagined in 2010) are shown in Figure 12 [5].

In the next 16 years, the size of Si trackers will increase neither in the HL-LHC detectors nor in the planned International Linear Collider (ILC) at CERN. It is assumed that silicon high granularity calorimeters (HGC) with an area of $\sim 1000\,\mathrm{m}^2$ will be created, and the implementation of a tracker for the future collider at CERN (Future Circular Collider, FCC) with a surface area of $\sim 400\,\mathrm{m}^2$ after completion of the HL-LHC operation is also discussed.

In the gamma-ray astrophysics, the only telescope currently containing silicon sensors is the LAT, whose tracker has a fairly small volume. However, the successful operation of the telescope for 16 years has shown the prospects of using Si sensors, which is reflected in plans to create future observatories that include more advanced and large-volume silicon trackers to study gamma-ray sources in the Universe.

As for the investigation of dark matter and neutrinos, the plans for the use of silicon are associated with the development of investigations by the international CDMS collaboration and within the framework of the Russian NCPM program. In the latter it is assumed that the weight of silicon will be 160 kg, and, of course, its implementation will make it possible to build a silicon megadetector for nuclear physics. The results achieved in the development of silicon sensors and the existing technological base give reason to believe that extensive plans in this area will be implemented.

Conflict of interest

The authors declare that they have no conflict of interest.

References

[1] https://home.cern
[2] M.J.G. Veltman. Facts and Mysteries in Elementary Particles Physics. World Scientific Publishing Co Pte., Singapore (copyright 2018). 340 p.
[3] J. Kemmer. Nucl. Instrum. Meth. **169**, *3*, 499 (1980).
[4] S. Ramo. Proceed. IRE **27**, *9*, 584 (1939).
[5] F. Hartmann. Evolution of Silicon Sensor Technology in Particle Physics, 2nd ed. Springer Tracts in Modern Physics 275. Springer Intern. Publishing AG (2017). 372 p.
[6] Yu.K. Akimov. Semiconductor nuclear radiation detectors. Dubna, JINR (2009). 277 p. (in Russian).
[7] G. Lutz. Semiconductor Radiation Detectors. Springer Berlin, Heidelberg (2007). 353 p.
[8] Particle Physics Reference Library, v. 2: Detectors for Particles and Radiation / Eds C.W. Fabjan, H. Schopper. Springer Open (2020). 1078 p.
[9] G.F. Knoll. Radiation Detection and Measurement, 4th ed. John Wiley, Hoboken, NJ (2010). 801 p.
[10] J. Lutz, H. Schlangenotto, U. Scheuermann, R. De Doncker. Semiconductor Power Devices: Physics, Characteristics, Reliability. Springer Berlin, Heidelberg (2011). 536 p.
[11] B.J. Baliga. Fundamentals of Power Semiconductor Devices. Springer Science+Business Media LLC, USA (2008). 1069 p.
[12] E.V. Verbitskaya, V.K. Eremin, N.N. Safonova, I.V. Eremin, Yu.V. Tuboltsev, S.A. Golubkov, K.A. Konkov. Semiconductors **45**, *4*, 536 (2011).
[13] G. Casse, P.P. Allport, T.J.V. Bowcock, A. Greenall, M. Hanlon, J.N. Jackson. Nucl. Instrum. Meth. A **487**, *3*, 465 (2002).
[14] G. Pellegrini, C. Fleta, F. Campabadal, M. Miñano, M. Lozano, J.M. Rafi, M. Ullán. Nucl. Instrum. Meth. A **579**, *2*, 599 (2007).
[15] V.A. Mitsou. arXiv:hep-ph/0004161v1 (2020).
[16] P.S. Miyagawa, I. Dawson. Radiation background studies for the phase II inner tracker upgrade. CERN, Tech. Rep. ATL-UPGRADE-PUB-2014-003 (2014).
[17] T. Szumlak. Nucl. Instrum. Meth. A **958**, 162187 (2020).
[18] The ATLAS Collaboration. arXiv:2407.05716v1 [physics.ins-det] 8 Jul 2024, CERN-EP-2024-156, 9th July (2024).
[19] X. Jia. Nucl. Instrum. Meth. A **1063**, 169236 (2024).

[20] V. Schönfelder, H. Aarts, K. Bennett, H. de Boer, J. Clear, W. Collmar, A. Connors, A. Deerenberg, R. Diehl, A. von Dordrecht, J.W. den Herder, W. Hermsen, M. Kippen, L. Kuiper, G. Lichti, et al. Astrophys. J. Suppl. Series **86**, 657 (1993).
[21] W.B. Atwood, A.A. Abdo, M. Ackermann, W. Althouse, B. Anderson, M. Axelsson, L. Baldini, J. Ballet, D.L. Band, G. Barbiellini, J. Bartelt, D. Bastieri, B.M. Baughman, K. Bechtol, D. Bédérède, et al. Astrophys. J. **697**, *2*, 1071 (2009).
[22] M. Ajello, W.B. Atwood, M. Axelsson, R. Bagagli, M. Bagni, L. Baldini, D. Bastieri, F. Bellardi, R. Bellazzini, E. Bissaldi, E.D. Bloom, R. Bonino, J. Bregeon, A. Brez, P. Bruel, et al. arXiv:2106.12203v3 [astro-ph.IM] 6 Sep 2021.
[23] S. Griffin. arXiv:1902.09380v1 [astro-ph.IM] 25 Feb 2019.
[24] A. De Angelis, V. Tatischeff, I.A. Grenier, J. McEnery, M. Mallamaci, M. Tavani, U. Oberlack, L. Hanlon, R. Walterm, A. Argan, P. VonBallmoos, A. Bulgarelli, A. Bykov, M. Hernanz, G. Kanbach, et al. J. High Energy Astrophys. **19**, 1 (2018).
[25] C.A. Kierans, the AMEGO Team. arXiv:2101.03105v1 [astro-ph.IM] 8 Jan (2021).
[26] D.W. Amaral, T. Aralis, T. Aramaki, I.J. Arnquist, E. Azadbakht, S. Banik, D. Barker, C. Bathurst, D.A. Bauer, L.V.S. Bezerra, R. Bhattacharyya, T. Binder, M.A. Bowles, P.L. Brink, R. Bunker, et al. Phys. Rev. D **102**, 091101(R) (2020).
[27] A.A. Yukhimchuk, A.N. Golubkov, I.P. Maksimkin, I.L. Malkov, O.A. Moskalev, R.K. Musyaev, A.A. Selezenev, L.V. Grigorenko, V.N. Trofimov, A.S. Fomichev, A.V. Golubeva, V.N. Verbetskii, K.A. Kuzakov, S.V. Mitrokhin, A.I. Studenikin, A.P. Ivashkin, I.I. Tkachev. FIZMAT **1**, *1*, 5 (2023). (in Russian).
[28] B.S. Neganov, V.N. Trofimov. Method of calorimetric measurement of ionizing radiation, USSR patent No. 1037771. (in Russian).
[29] V. Eremin, A. Shepelev, E. Verbitskaya, C. Zamantzas, A. Galkin. J. Appl. Phys. **123**, *20*, 204501 (2018).
[30] E.M. Verbitskaya, I.V. Eremin, A.A. Podoskin, V.O. Zbrozhek, S.O. Slipchenko, N.N. Fadeeva, A.A. Yablokov, V.K. Eremin. FTP **58**, *8*, 415 (2024). (in Russian).

Translated by A.Akhtyamov